Published in final edited form as:
Neuroimage. 2012 January 16; 59(2): 887–894. doi:10.1016/j.neuroimage.2011.09.065.

White matter integrity deficits in prefrontal-amygdala pathways in Williams syndrome

Suzanne N. Avery[1], **Tricia A. Thornton-Wells**[2,3,4,7], **Adam W Anderson**[4,5,6,7], and **Jennifer Urbano Blackford**[4,8,9]

[1]Vanderbilt Brain Institute, Neuroscience Graduate Program, Vanderbilt University, Nashville, TN

[2]Center for Human Genetics Research, Vanderbilt University Medical Center, Nashville, TN

[3]Department of Molecular Physiology and Biophysics, Vanderbilt University, Nashville, TN

[4]Vanderbilt Kennedy Center for Research on Human Development, Vanderbilt University, Nashville, TN

[5]Department of Radiology and Radiological Sciences, Vanderbilt University, Nashville, TN

[6]Department of Biomedical Engineering, School of Engineering, Vanderbilt University, Nashville, TN

[7]Vanderbilt University Institute of Imaging Science, Vanderbilt University, Nashville, TN

[8]Department of Psychiatry, Vanderbilt University School of Medicine, Nashville, TN

[9]Department of Psychology, Vanderbilt University, Nashville, TN

Abstract

Williams syndrome is a neurodevelopmental disorder associated with significant non-social fears. Consistent with this elevated non-social fear, individuals with Williams syndrome have an abnormally elevated amygdala response when viewing threatening non-social stimuli. In typically-developing individuals, amygdala activity is inhibited through dense, reciprocal white matter connections with the prefrontal cortex. Neuroimaging studies suggest a functional uncoupling of normal prefrontal-amygdala inhibition in individuals with Williams syndrome, which might underlie both the extreme amygdala activity and non-social fears. This functional uncoupling might be caused by structural deficits in underlying white matter pathways; however, prefrontal-amygdala white matter deficits have yet to be explored in Williams syndrome. We used diffusion tensor imaging to investigate prefrontal-amygdala white matter integrity differences in individuals with Williams syndrome and typically-developing controls with high levels of non-social fear. White matter pathways between the amygdala and several prefrontal regions were isolated using probabilistic tractography. Within each pathway, we tested for between-group differences in three measures of white matter integrity: fractional anisotropy (FA), radial diffusivity (RD), and parallel diffusivity (λ_1). Individuals with Williams syndrome had lower FA, compared to controls, in several of the prefrontal-amygdala pathways investigated, indicating a reduction in white matter integrity. Lower FA in Williams syndrome was explained by significantly higher RD, with no

Corresponding Author: Jennifer Urbano Blackford, Vanderbilt Department of Psychiatry, 1601 23rd Avenue South, Suite 3057J, Nashville, TN 37212, Phone: 615.343.0715, Jennifer.Blackford@Vanderbilt.edu, Web: www.blackfordlab.com.

differences in λ_1, suggestive of lower fiber density or axon myelination in prefrontal-amygdala pathways. These results suggest that deficits in the structural integrity of prefrontal-amygdala white matter pathways might underlie the increased amygdala activity and extreme non-social fears observed in Williams syndrome.

Keywords

diffusion tensor imaging; fear; neurodevelopmental disorders; genetics

Introduction

Williams syndrome (OMIM#194050) is a rare neurodevelopmental disorder caused by a microdeletion of about 25 genes on chromosome 7 (band 7q11.23) (Ewart et al., 1993). Individuals with Williams syndrome (WS) are socially fearless and disinhibited (Doyle et al., 2004; Dykens, 2003; Gosch and Pankau, 1994), yet intriguingly, have unusually high levels of non-social fears (Dykens, 2003; Klein-Tasman and Mervis, 2003; Leyfer et al., 2006; Stinton et al., 2010). These non-social fears increase in severity with age (Davies et al., 1998; Dykens, 2003) and result in intense anticipatory anxiety which significantly impairs daily functioning (Dykens, 2003). Accordingly, around 50% of individuals with WS have a comorbid diagnosis of specific phobia (Leyfer et al., 2009; Leyfer et al., 2006), compared to an estimated specific phobia prevalence of 4–9% in the general population (American Psychiatric Association, 1994; Kessler et al., 2005). Given significant clinical impairment, it is imperative to understand the unique neurobiology which underlies elevated non-social fear in individuals with WS.

The amygdala—a small subcortical structure involved in threat detection and fear processing (Aggleton, 2000)—is involved in abnormal fear processing in individuals with WS (Bellugi et al., 1999; Reiss et al., 2004). When viewing threatening non-social scenes, individuals with WS exhibit elevated amygdala activity compared to typically-developing controls (Meyer-Lindenberg et al., 2005; Munoz et al., 2010). Interestingly, this increased amygdala activity appears to be above and beyond what can be accounted for by normal fear processing; individuals with WS exhibit elevated amygdala activity in response to threatening non-social scenes even when compared to controls matched for a level of nonsocial fear (Thornton-Wells et al., 2011). This amygdala hyperactivity suggests a difference in neural processing in individuals with WS that is unique to WS as a disorder and that cannot be accounted for by a high trait level of non-social fear. Despite this extreme amygdala response to threatening non-social stimuli, individuals with WS do not have chronically elevated amygdala activity to all types of stimuli (Meyer-Lindenberg et al., 2005; Thornton-Wells et al., 2011), indicating that amygdala hyperactivity in response to threatening non-social stimuli is not simply due to global functional impairment of the amygdala. Instead, amygdala hyperactivity in WS might result from a lack of cortical inhibitory control within the context of non-social threat.

Amygdala hyperactivity may result from a failure of the orbitofrontal cortex (OFC) to properly inhibit amygdala responses during non-social fear processing. The OFC sends dense axonal projections to the amygdala (Stefanacci and Amaral, 2002) which synapse within primarily GABAergic nuclei (Ghashghaei and Barbas, 2002), suggesting an inhibitory role for OFC inputs. In agreement with anatomical evidence, previous neuroimaging studies have demonstrated that the OFC plays a role in top-down regulation of amygdala response and emotional reactivity in typically-developing individuals (Indovina et al., 2011; Ochsner et al., 2004; Phan et al., 2005). In individuals with WS, normal OFC inhibition of the amygdala is disrupted (Meyer-Lindenberg et al., 2005). These findings

suggest circuit-level impairment of normal OFC-amygdala inhibition in the context of non-social fear processing, which may result in amygdala hyperactivity in individuals with WS.

Another prefrontal cortex region, the subgenual anterior cingulate cortex (sgACC), may also inhibit amygdala responses (Pezawas et al., 2005). The sgACC receives dense structural projections from the amygdala (Freedman et al., 2000) and is implicated as a key neural substrate underlying anxiety and negative emotions (Drevets et al., 1997; Liotti et al., 2000; Ongur et al., 1998). Dysfunction in the sgACC might contribute to pathological fear processes; for example, individuals at high risk for development of anxiety disorders have increased amygdala activity in response to fearful stimuli (Hariri et al., 2002; Hariri et al., 2005), decreased sgACC volume (Pezawas et al., 2005), and decreased functional coupling between sgACC and the amygdala (Pezawas et al., 2005). Although the function of the sgACC has not been specifically explored in WS, two previous structural studies have demonstrated significantly lower gray matter density in the sgACC region in individuals with WS compared to controls (Campbell et al., 2009; Chiang et al., 2007). Given the role of the sgACC in anxiety, decreased gray matter density in the sgACC region in WS provides intriguing evidence that disrupted sgACC-amygdala interaction might contribute to abnormal amygdala hyperactivity during non-social fear contexts.

While converging lines of evidence point toward a functional disconnect in normal prefrontal-amygdala inhibition during non-social fear processing in WS, the underlying structural mechanisms remain unclear. One potential mechanism is reduced structural integrity of the axons which form prefrontal-amygdala inhibitory pathways. Individuals with WS show marked abnormalities in widespread white matter pathways (Hoeft et al., 2007; Marenco et al., 2007). While some white matter abnormalities observed in WS have been specifically associated with discrete neurocognitive impairments (Hoeft et al., 2007), to date, no studies have directly investigated whether structural integrity deficits in prefrontal-amygdala white matter pathways might contribute to abnormal non-social fear processing in WS.

In the present study, we used diffusion tensor imaging (DTI) to investigate prefrontal-amygdala white matter integrity in individuals with WS relative to controls. To isolate structural deficits unique to WS and not due to high non-social fear, we targeted a control group that was also high in non-social fear but did not have WS. We hypothesized that individuals with WS, compared to controls, would show structural abnormalities in white matter pathways between prefrontal inhibitory control regions, including the OFC and sgACC, and the amygdala.

Methods

Participants

Eight individuals with Williams syndrome and 10 typically-developing control individuals participated in this study. One control subject was removed from analysis due to excessive motion during the DTI acquisition (excessive motion was defined as translational motion > 4 mm or rotational motion > 3 degrees), resulting in a group of 9 control subjects included in data analysis. Subjects were 19‰38 years old (mean = 23 years) and were predominantly Caucasian (88%) and right handed (71%) (Table 1).

WS subjects were recruited through an existing database of persons who had either attended or expressed interest in the Vanderbilt Kennedy Center WS Music Camp. In order to isolate white matter structural deficits unique to WS rather than non-social fear, we recruited a control group that was high in non-social fear but did not have WS. Control subjects were recruited through advertisements targeting healthy individuals in the general population who

were “especially shy” as children, and through research participant databases. We selected a control group with inhibited temperament; inhibited temperament is a trait characterized by social fears and shyness (Kagan et al., 1988) as well as significant non-social fears (Biederman et al., 1990; Goodwin et al., 2004; Smoller et al., 2005), and individuals with inhibited temperament are at significantly increased risk for development of anxiety disorders, similar to individuals with WS (Chronis-Tuscano et al., 2009; Essex et al., 2010; Schwartz et al., 1999).

Control subjects completed two temperament screening questionnaires as a prerequisite for study inclusion: the Retrospective Self-Report of Inhibition (RSRI; Reznick et al., 1992) and the Adult Self-Report of Inhibition (ASRI; Reznick et al., 1992). Both the RSRI and ASRI have good reliability and construct validity (Reznick et al., 1992). The RSRI and ASRI are comprised of social and non-social subscales, which provide information on inhibition in the social and non-social realms. These subscales were critical for the current study because they allowed us to select control subjects who demonstrated high levels of non-social inhibition. High trait level of non-social inhibition was defined as having scores within the top 15% on both the RSRI and ASRI non-social subscales, based on normative data from the general population (Reznick et al., 1992). WS subjects also completed both the RSRI and ASRI in order to characterize their level of non-social inhibition, but were not selected for the study based on these scores. As expected, both subject groups reported high levels of trait non-social inhibition (Table 1). However, it should be noted that individuals with WS did not self-report extreme levels of childhood non-social inhibition, which may be due to either issues with retrospective self-report in WS or age-related increases in levels of non-social fear.

Subjects in both groups were excluded on the basis of: failure to pass MRI safety screen, substance abuse or dependence in the past 6 months, presence of severe psychiatric illness (such as schizophrenia or bipolar disorder), prior head injury, significant medical illness (e.g. HIV, cancer), claustrophobia or pregnancy. Psychopathology was assessed in all subjects by a trained interviewer using the Structured Clinical Interview for the DSM-IV (SCID I-P; First et al., 2002). Subjects were not excluded for the presence of anxiety or depression because both are common in individuals with WS (Dykens, 2003; Stinton et al., 2010) and in extreme inhibited temperament (Schwartz et al., 1999). One individual with WS was diagnosed with an anxiety disorder (panic disorder-past); two controls were diagnosed with the following disorders (major depressive disorder-past (n=1), social phobia-current (n=1)). Similarly, we did not exclude subjects for use of psychoactive medications because individuals with WS often take medication to control their anxiety. IQ was assessed using the Kaufmann Brief Intelligence Test, Second Edition (Kaufman and Kaufman, 1990). Handedness was assessed using the Edinburgh Handedness Inventory (Oldfield, 1971). A full clinical characterization of a largely overlapping set of individuals who participated in a functional MRI task has previously been published (Thornton-Wells et al., 2011).

The Vanderbilt University Institutional Review Board approved the study. Written informed consent was obtained after providing subjects with a complete description of the study. For subjects with WS, a parent or guardian also provided written informed consent.

Demographic Data Analysis

Due to non-normality of some measures, nonparametric Wilcoxon Mann-Whitney tests were used to characterize between-group differences in temperament, IQ, and age. Chi-Square tests were used to characterize between-group differences in gender, handedness, race, and psychiatric diagnoses (Table 1). A p-value of .05 was used for all analyses. Data were analyzed using SPSS (SPSS Statistics 18 for Windows, 2010, version 18.0.2).

Image Acquisition

Diffusion weighted images, T1-weighted anatomical MRI images, and B_0 field inhomogeneity maps were collected on a 3 Tesla Philips Achieva MRI scanner (Philips Healthcare, Inc., Best, The Netherlands) at the Vanderbilt University Institute of Imaging Science. Whole-brain diffusion weighted images were acquired using an 8-channel SENSE head coil. Diffusion weighted data were acquired using an echoplanar multislice single-shot spin echo pulse sequence and the following parameters: FOV = 256×256; TE/TR = 60/10000 ms; flip angle = 90°; voxel size = 2 mm isotropic; number of slices = 60. We acquired 32 diffusion directions with a *b* value of 1000 s/mm^2 and one T2-weighted volume with a *b* value of 0 s/mm^2. High resolution T1-weighted anatomical images were collected with the following parameters: FOV = 256 mm; number of slices = 170; voxel size = 1 mm isotropic; gap = 0 mm. B_0 field inhomogeneity maps were collected with the following parameters: FOV = 240 mm; TE/TR = 3.38/393 ms; flip angle = 90°; number of slices = 36; voxel size = 2.5 mm isotropic.

Data Preprocessing

Diffusion weighted data were pre-processed using the FMRIB Software Library (FSL, version 4.1.4; Oxford Centre for Functional MRI of the Brain (FMRIB), UK; http://www.fmrib.ox.ac.uk/fsl/) (Behrens et al., 2003; Smith et al., 2004) and Matlab (Version R2010, The MathWorks, Inc, Natick, MA). Diffusion data were: corrected for eddy current distortions and motion using the Eddy Current Correction tool within the FMRIB FDT toolbox (version 2.0); corrected for geometric distortions caused by B_0 field inhomogeneities using custom Matlab-based scripts; skull stripped using the FMRIB Brain Extraction tool (BET; Smith, 2002); and visually inspected for artifacts. Diffusion tensors were fitted at each voxel using the FMRIB FDT toolbox and fractional anisotropy (FA), radial diffusivity [RD = $(\lambda_2 + \lambda_3) / 2$], and parallel diffusivity (λ_1) maps were calculated for statistical analysis.

Probabilistic Tractography Analysis

Probabilistic fiber tractography was used to identify prefrontal-amygdala white matter pathways. Probabilistic fiber tractography was performed using the FMRIB FDT toolbox, which allows for estimation of the most probable location of a pathway between two seed points using Bayesian techniques (Behrens et al., 2003; Jbabdi et al., 2007; Smith et al., 2004). Probabilistic tractography was performed ipsilaterally from the amygdala to each of five cortical regions (and vice versa) for each hemisphere, resulting in 10 separate tractography pathways for each subject (Fig. S1). A multi-seed-mask approach, in which anterograde and retrograde amygdala tracts were summed together, was used to robustly characterize each prefrontal-amygdala tract. Fiber tracking was initiated from all voxels within each seed mask (5000 streamline samples per seed voxel, 0.5 mm step lengths, curvature threshold = 0.2). The following anatomical seed masks were used: amygdala, subgenual anterior cingulate (BA25), inferior orbitofrontal cortex (infOFC), medial orbitofrontal cortex (medOFC), middle orbitofrontal cortex (midOFC), and superior orbitofrontal cortex (supOFC) (Fig. S2). To account for inter-individual variability in amygdala shape and volume, amygdala seed masks were created individually by segmenting each subject's T1-weighted image using automated routines implemented by FreeSurfer. FreeSurfer segmentations were carefully reviewed to ensure the accuracy of these masks. Because the subgenual anterior cingulate region has relatively poorly defined borders, we selected a Brodmann area (BA25) located centrally within the subgenual anterior cingulate region. The BA25 cortical seed mask was derived from the Talairach Daemon database (Lancaster et al., 1997; Lancaster et al., 2000) within the WFU Pickatlas (Wake Forest University Pickatlas; Maldjian et al., 2003; Maldjian et al., 2004). The remaining cortical seed masks (infOFC, medOFC, midOFC, and supOFC) were derived from the AAL brain

atlas (Automated Anatomical Labeling; Tzourio-Mazoyer et al., 2002) within the WFU Pickatlas. To constrain tractography streamlines within ipsilateral white matter, we used an explicit FA mask thresholded at FA > .2 combined with a midline exclusion mask. Quality control analyses of prefrontal-amygdala tracts were performed (see Supplementary Methods).

In order to test for between-group differences in the white matter integrity, voxelwise statistics were performed within each of the prefrontal-amygdala tracts. Tests for between-group differences were conducted using general linear models (two sample t-tests) with p-values estimated using permutation testing (FMRIB Randomise tool; 5,000 permutations). Statistical significance was determined by a cluster-forming threshold of $t > 2$ and a voxel-level $p < 0.05$, family-wise error corrected for multiple comparisons. In order to identify the specific anatomical pathways where FA differences were located, significant FA differences were overlaid onto probabilistic anatomical white matter atlases (Eickhoff et al., 2005; Eickhoff et al., 2006; Eickhoff et al., 2007; Hua et al., 2008; Mori et al., 2004; Wakana et al., 2007) in FSL. To aid in interpretation of any between-group FA differences, post-hoc analyses of RD and λ_1 were performed. Mean RD and λ_1 values for each subject were extracted from significant FA clusters and analyzed using non-parametric Wilcoxon Mann-Whitney tests within SPSS. A p-value of .05 was considered significant.

Voxelwise Analysis Using Tract-Based Spatial Statistics

In addition to testing for differences in prefrontal-amygdala pathways, our *a priori* regions of interest, we also conducted whole-brain voxelwise statistical analyses of FA data using tract-based spatial statistics (TBSS, version 1.2; Smith et al., 2006). TBSS uses automated routines to calculate a white matter skeleton which represents the center of each white matter tract, and all subsequent voxelwise analyses are performed within the spatial extent of the TBSS skeleton. Two advantages of the TBSS skeleton over whole-brain voxelwise statistics are that it minimizes errors in coregistration between subjects and also minimizes the effects of white matter lesions on group coregistration. The details of the TBSS skeleton creation are presented in the Supplementary Methods.

Between-group voxelwise differences were examined using general linear models (two sample t-tests) with p-values estimated using permutation testing (as described in the probabilistic tractography analysis). Because between-group differences were widespread, we used a restrictive statistical threshold with a cluster-forming threshold of $t > 3$ and a voxel-level $p < 0.05$, family-wise error corrected for multiple comparisons, to allow us to identify separable clusters. Post-hoc analyses of mean RD and λ_1 values within significant FA clusters were conducted using non-parametric Wilcoxon Mann-Whitney tests within SPSS. A p-value of .05 was considered significant.

Global White Matter Analysis of Mean Diffusion Characteristics

We conducted global analyses of diffusion data (FA, RD, and λ_1) to examine potential gross, overall differences in white matter diffusion characteristics. In order to isolate only white matter voxels, each subject's diffusion data were masked using their T1-derived white matter segmentation (white matter segmentation performed using FreeSurfer version 4.5.0; http://surfer.nmr.mgh.harvard.edu/) (Fischl et al., 2002). Each subject's mean white matter value for each diffusion measure was calculated using the FMRIB fslstats tool. Between-group non-parametric Wilcoxon Mann-Whitney tests were conducted using SPSS. Differences were considered significant at $p < 0.05$.

Results

Prefrontal-Amygdala Pathway Analysis

To determine whether individuals with WS had decreased white matter integrity in prefrontal-amygdala pathways, we compared FA within tracts identified by probabilistic tractography. Individuals with WS had significantly lower FA in regions of several of the tracts tested (bilateral BA25-to-amygdala, bilateral infOFC-to-amygdala, right medOFC-to-amygdala, and right supOFC-to-amygdala), indicating extensive differences in prefrontal-amygdala white matter integrity. There were no group differences in the midOFC-amygdala tract. In order to identify the specific anatomical pathways where individuals with WS had significantly lower FA than controls, we overlaid significant FA differences onto probabilistic anatomical white matter atlases. Individuals with WS had significantly lower FA than control subjects within bilateral ventral amygdalofugal pathways, bilateral uncinate fasciculi (UF), bilateral inferior longitudinal fasciculi (ILF), and right inferior fronto-occipital fasciculus (IFO) (Table 2; Fig. 1; Fig. S3; Fig. S4).

Radial diffusivity (RD) and parallel diffusivity (λ_1), each a subcomponent of FA, are estimates of the extent of water diffusion perpendicular to the fiber bundle (RD) and the extent of water diffusion along the length of the fiber bundle (λ_1), respectively. Because FA values can be reduced due to an increase in RD, a decrease in λ_1, or some combination of each, we performed post-hoc between-group analyses of mean RD and λ_1 values within regions of significant FA differences. Individuals with WS had significantly larger mean RD than control subjects within regions of significant FA differences (RD, $p < .001$). Further investigation of RD differences revealed significantly larger mean RD in individuals with WS in each of the tracts tested (Fig. S5; Fig. S6). However, individuals with WS and controls had similar mean parallel diffusivity (λ_1, $p = .923$), suggesting that the FA differences were not the result of decreased water diffusion along the length of the prefrontal-amygdala pathways. Taken together, these findings suggest that FA is lower in WS due to an increase in water diffusion perpendicular to prefrontal-amygdala pathways.

Next, we tested for areas where prefrontal-amygdala FA was higher in individuals with WS. Individuals with WS had significantly higher FA than controls in a region of the right midOFC-to-amygdala tract. In order to identify the specific anatomical pathway, we overlaid the significant FA cluster onto probabilistic anatomical white matter atlases. The area of higher FA was located in the right IFO (Table 2; Fig. 1). In order to investigate the underlying cause of higher FA values in WS, we conducted post-hoc analyses of mean RD and λ_1 values within the region where individuals with WS demonstrated higher FA values than controls. Individuals with WS had significantly smaller mean RD (RD, $p = .021$; Fig. S7) and larger mean λ_1 (λ_1, $p = .016$; Fig. S7) than controls within the region of significant FA differences, indicating that individuals with WS had less water diffusion perpendicular to the fiber bundles and greater diffusion parallel to the fiber than controls within this regions. This finding suggests that FA is higher in certain regions in individuals with WS due to a decrease in water diffusion perpendicular to fiber bundles, along with a corresponding increase in parallel diffusivity within these regions.

Whole-Brain White Matter Analyses

To test for white matter integrity differences across the whole brain, we compared FA values between individuals with WS and controls within the center of white matter pathways using TBSS. Individuals with WS had significantly lower FA than controls in widespread white matter tracts, including: left ventral amygdalofugal pathway; right uncinate fasciculus (UF); the genu, body and splenium of the corpus callosum (CC); anterior commissure (AC); bilateral posterior limbs of the internal capsule (PLIC); bilateral external capsules (EC); left

inferior fronto-occipital fasciculus (IFO); and left cortico-spinal tract (CST) (Fig. 2). Importantly, TBSS findings in the ventral amygdalofugal pathway and uncinate fasciculus replicate tractography findings (Fig. 2, inset). Individuals with WS did not have significantly higher FA in any white matter tract when compared to controls.

To further investigate the components contributing to widespread decreased FA in WS, we performed post-hoc between-group analyses of mean RD and λ_1 within regions of FA differences. Consistent with tractography findings, individuals with WS had significantly higher mean RD values in areas of significant FA differences (RD, $p = 0.005$; Fig. S7), indicating an overall increase in water diffusion perpendicular to fiber bundles in WS. Mean λ_1 values were lower in individuals with WS, compared to controls, in areas where FA differences were observed (λ_1, $p = 0.005$; Fig. S8), indicating a general decrease in water diffusion along the length of fiber bundles in WS. Together, these results indicate that general white matter integrity deficits in WS are the result of both decreased diffusion along the length of fiber bundles and increased diffusion perpendicular to fiber bundles.

Finally, to examine potential gross, overall differences in white matter diffusion characteristics, we compared mean global diffusion across groups. When comparing mean diffusion across all white matter, individuals with WS did not have significantly different diffusion characteristics relative to controls (FA, $p = .248$; λ_1, $p = .386$; RD, $p = .700$; Fig. S9), suggesting that the observed prefrontal-amygdala differences are not indicative of widespread reductions in white matter integrity. Instead, the white matter integrity differences detected in voxelwise analyses (tractography-ROI and TBSS) in individuals with WS are likely limited to specific regions within white matter tracts.

Discussion

To test for structural differences in prefrontal-amygdala white matter pathways in Williams syndrome (WS), we compared white matter integrity in individuals with WS to typically-developing controls matched for high trait levels of non-social fear. Findings from two analytic methods, probabilistic tractography and Tract-Based Spatial Statistics (TBSS), both demonstrated decreased white matter integrity in prefrontal-amygdala white matter paths in individuals with WS. Because the prefrontal cortex plays an important role in inhibition of amygdala activity, we propose that these white matter integrity deficits are a critical component underlying both amygdala hyperactivity and increased non-social fear in individuals with WS.

In this study, we demonstrate decreased white matter integrity in orbitofrontal cortex (OFC)-amygdala white matter pathways in WS. Our findings provide initial evidence for a structural mechanism which might underlie the OFC-amygdala functional disconnect previously shown in individuals with WS (Meyer-Lindenberg et al., 2005). In typically-developing individuals, activity in the OFC is negatively correlated with both amygdala activity and fear-related physiological arousal. For example, passive viewing of negative scenes results in increased amygdala activity in healthy participants; however, when individuals are instructed to suppress their emotional response to negative scenes, lateral OFC activity increases while amygdala activity reduces to baseline (Ochsner et al., 2004; Phan et al., 2005). OFC activity is also negatively correlated with fear-related physiological arousal (Indovina et al., 2011). However, in individuals with WS, the OFC fails to show normal functional activation in response to fearful faces (Meyer-Lindenberg et al., 2005) and threatening scenes (Munoz et al., 2010). Individuals with WS also show a functional disconnect in normal OFC-amygdala interaction, with the OFC failing to show typical modulatory interactions with the amygdala (Meyer-Lindenberg et al., 2005). We speculate

that white matter structural deficits in OFC-amygdala pathways may underlie the altered functional connectivity found in individuals with WS.

Our findings also show white matter integrity deficits in the subgenual anterior cingulate cortex (sgACC)-amygdala tract in WS. Although functional interactions between the sgACC and the amygdala have not previously been investigated in WS, Pezawas and colleagues (2005) have shown decreased functional coupling between the sgACC and amygdala in adults with genetic risk for anxiety. Pezawas and colleagues proposed a modulatory feedback circuit where the amygdala activates the sgACC, which in turn activates the dorsal ACC, which completes an inhibitory feedback loop to the amygdala. Altered sgACC-amygdala white matter integrity in individuals with WS might disrupt feedback inhibition of the amygdala through this circuit. The sgACC has also been prominently implicated in anxiety and depression (Drevets et al., 1997; Liotti et al., 2000; Ongur et al., 1998). Volume in the sgACC is decreased in both individuals with genetic risk for anxiety (Pezawas et al., 2005) and individuals with WS (Campbell et al., 2009; Chiang et al., 2007). Given the increased non-social anxiety in individuals with WS, we speculate that disruption in the sgACC-amygdala white matter tract might contribute to both increased amygdala activation and increased non-social anxiety observed in individuals with WS.

In addition to the major findings of reduced FA in WS, there was an area of increased FA in WS within the inferior fronto-occipital fasciculus, a major longitudinal pathway. A similar finding has been previously reported (Marenco et al., 2007) and this finding is consistent with a hypothesis set forth by Marenco and colleagues (2007) based on the genes commonly deleted in WS. Previous studies have identified two genes typically deleted in WS—LIMK1 and CYLN2—that are thought to be essential for growth cone regulation and therefore might play a role in axon guidance (Merla et al., 2010). In line with a neurodevelopmental deficit in axon guidance cues, Marenco and colleagues (2007) proposed that some axons which would normally form U shaped pathways would fail to turn and instead follow longitudinal guidance cues, resulting in: fewer U shaped fibers crossing the dorsal corpus callosum; increased axon number; increased axon coherence in longitudinal white matter pathways; and aberrant pathways. Consistent with this model, we found that individuals with WS had decreased corpus callosum white matter integrity, increased whole-brain radial diffusivity (which may correspond to a decreased number of axons), and higher FA in the inferior fronto-occipital fasciculus, a major longitudinal pathway. When we further investigated the region of higher FA in WS, we found that WS subjects had both increased parallel diffusivity and decreased radial diffusivity, which is in line with an increase in axon number and axon coherence in this pathway compared to controls. Intriguingly, the region of increased FA in WS is located near the edge of the inferior fronto-occipital fasciculus rather than at its center, and is likely in a transitional region between gray and white matter where there are few longitudinal fibers in typical individuals. This may suggest the presence of an aberrant or abnormally expanded pathway in WS; future studies should specifically investigate the possible presence of aberrant pathways in this region of the inferior fronto-occipital fasciculus.

Although WS was associated with widespread integrity deficits at the center of white matter tracts in our exploratory whole-brain TBSS analysis, global white matter integrity (averaged across the whole brain) was comparable between groups. This finding is in contrast to a previous study which showed that individuals with WS had a small (~5%) but significant global reduction in trace, a marker of white matter integrity (Marenco et al., 2007). However, studies investigating specific white matter pathways in WS have shown a combination of decreased (Marenco et al., 2007) and increased (Hoeft et al., 2007; Marenco et al., 2007) white matter coherence. Although we found widespread decreases in white matter integrity, we also found small regions of significantly increased FA values in the

prefrontal cortex in our WS group. Therefore, our finding of non-significant global differences in white matter integrity might reflect that individuals with WS have both widespread decreased and regionally increased white matter integrity.

A limitation of this study is the small sample size. While the reported prefrontal-amygdala white matter integrity findings are relatively large, consistent across two analysis methods, and in line with previous findings in individuals with WS, they should be interpreted with caution due to the small sample size. Another limitation of this study is that, due to widespread white matter alterations in WS, we cannot rule out the possibility that our white matter findings are incidental. Multimodal imaging studies in larger cohorts are needed to replicate these structural findings and explicitly explore structure-function relationships in individuals with WS. Another limitation of this study is the potential presence of geometric distortions, due to field inhomogeneities, within our prefrontal white matter tracts of interest; although, we reduced the impact of geometric distortions on our data by correcting images using b_0 field maps. Although the OFC has also been implicated in hypersociability in WS, we did not specifically explore or control for hypersociability in the present study. Future studies should systematically explore the differing roles of medial and lateral OFC on both hypersociability and increased non-social fear in WS. Additional research should also include WS individuals with atypical deletions to explore the contribution of specific genes on white matter development.

In conclusion, these findings are the first, to our knowledge, to demonstrate that individuals with WS have white matter integrity deficits in prefrontal-amygdala pathways. We speculate that these white matter deficits might underlie the amygdala hyperactivity and non-social fears seen in individuals with WS. Therefore, this study provides preliminary evidence for a neural mechanism for the extreme amygdala hyperactivity and non-social fears observed in WS.

Research Highlights

- Individuals with Williams syndrome (WS) show amygdala hyperactivity to threatening non-social images
- Amygdala activity is inhibited by prefrontal cortical regions in typically-developing adults
- Individuals with WS have decreased integrity in prefrontal-amygdala white matter pathways
- Deficits in prefrontal-amygdala white matter may contribute to amygdala hyperactivity in WS

Supplementary Material

Refer to Web version on PubMed Central for supplementary material.

Acknowledgments

We thank the individuals with Williams syndrome and their families for participating in this study. We thank Elizabeth Roof for research assistance. This research was supported in part by funding from the National Institute of Mental Health NIMH (K01-MH083052 to JUB), NIH Roadmap for Medical Research Postdoctoral Fellowship - Biobehavioral Intervention Training Program (T32 MH75883, TATW), a Hobbs Discovery Grant from the Vanderbilt Kennedy Center, the Vanderbilt Institute for Clinical and Translational Research (1-UL1-RR024975 NCRR/NIH), the Vanderbilt University Institute of Imaging Science, and the Vanderbilt Brain Institute Neuroscience Graduate Program.

Reference List

Aggleton, JP. 2nd ed.. New York: Oxford University Press; 2000. The Amygdala.

American Psychiatric Association. Washington, DC: American Psychiatric Association; 1994. Diagnostic and Statistical Manual of Mental Disorders, 4 (DSM-IV).

Behrens TE, Woolrich MW, Jenkinson M, Johansen-Berg H, Nunes RG, Clare S, Matthews PM, Brady JM, Smith SM. Characterization and propagation of uncertainty in diffusion-weighted MR imaging. Magn Reson.Med. 2003; 50:1077–1088. [PubMed: 14587019]

Bellugi U, Adolphs R, Cassady C, Chiles M. Towards the neural basis for hypersociability in a genetic syndrome. Neuroreport. 1999; 10:1653–1657. [PubMed: 10501552]

Biederman J, Rosenbaum JF, Hirshfeld DR, Faraone SV, Bolduc EA, Gersten M, Meminger SR, Kagan J, Snidman N, Reznick JS. Psychiatric correlates of behavioral inhibition in young children of parents with and without psychiatric disorders. Arch.Gen.Psychiatry. 1990; 47:21–26. [PubMed: 2294852]

Campbell LE, Daly E, Toal F, Stevens A, Azuma R, Karmiloff-Smith A, Murphy DG, Murphy KC. Brain structural differences associated with the behavioural phenotype in children with Williams syndrome. Brain Res. 2009; 1258:96–107. [PubMed: 19118537]

Chiang MC, Reiss AL, Lee AD, Bellugi U, Galaburda AM, Korenberg JR, Mills DL, Toga AW, Thompson PM. 3D pattern of brain abnormalities in Williams syndrome visualized using tensor-based morphometry. Neuroimage. 2007; 36:1096–1109. [PubMed: 17512756]

Chronis-Tuscano A, Degnan KA, Pine DS, Perez-Edgar K, Henderson HA, Diaz Y, Raggi VL, Fox NA. Stable early maternal report of behavioral inhibition predicts lifetime social anxiety disorder in adolescence. J.Am.Acad.Child Adolesc.Psychiatry. 2009; 48:928–935. [PubMed: 19625982]

Davies M, Udwin O, Howlin P. Adults with Williams syndrome. Preliminary study of social, emotional and behavioural difficulties. Br.J.Psychiatry. 1998; 172:273–276. [PubMed: 9614479]

Doyle TF, Bellugi U, Korenberg JR, Graham J. "Everybody in the world is my friend" hypersociability in young children with Williams syndrome. Am.J.Med.Genet.A. 2004; 124A:263–273. [PubMed: 14708099]

Drevets WC, Price JL, Simpson JR Jr, Todd RD, Reich T, Vannier M, Raichle ME. Subgenual prefrontal cortex abnormalities in mood disorders. Nature. 1997; 386:824–827. [PubMed: 9126739]

Dykens EM. Anxiety, fears, and phobias in persons with Williams syndrome. Dev.Neuropsychol. 2003; 23:291–316. [PubMed: 12730029]

Eickhoff SB, Heim S, Zilles K, Amunts K. Testing anatomically specified hypotheses in functional imaging using cytoarchitectonic maps. Neuroimage. 2006; 32:570–582. [PubMed: 16781166]

Eickhoff SB, Paus T, Caspers S, Grosbras MH, Evans AC, Zilles K, Amunts K. Assignment of functional activations to probabilistic cytoarchitectonic areas revisited. Neuroimage. 2007; 36:511–521. [PubMed: 17499520]

Eickhoff SB, Stephan KE, Mohlberg H, Grefkes C, Fink GR, Amunts K, Zilles K. A new SPM toolbox for combining probabilistic cytoarchitectonic maps and functional imaging data. Neuroimage. 2005; 25:1325–1335. [PubMed: 15850749]

Essex MJ, Klein MH, Slattery MJ, Goldsmith HH, Kalin NH. Early risk factors and developmental pathways to chronic high inhibition and social anxiety disorder in adolescence. Am.J.Psychiatry. 2010; 167:40–46. [PubMed: 19917594]

Ewart AK, Morris CA, Atkinson D, Jin W, Sternes K, Spallone P, Stock AD, Leppert M, Keating MT. Hemizygosity at the elastin locus in a developmental disorder, Williams syndrome. Nat.Genet. 1993; 5:11–16. [PubMed: 7693128]

First, M.; Spitzer, R.; Gibbon, M.; Williams, J. Biometrics Research. New York: New York State Psychiatric Institute; 2002. Structured Clinical Interview for DSM-IV-TR Axis I Disorders, Research Version, Patient Edition (SCID-I/P).

Fischl B, Salat DH, Busa E, Albert M, Dieterich M, Haselgrove C, van der Kouwe A, Killiany R, Kennedy D, Klaveness S, Montillo A, Makris N, Rosen B, Dale AM. Whole brain segmentation: automated labeling of neuroanatomical structures in the human brain. Neuron. 2002; 33:341–355. [PubMed: 11832223]

Freedman LJ, Insel TR, Smith Y. Subcortical projections of area 25 (subgenual cortex) of the macaque monkey. J.Comp Neurol. 2000; 421:172–188. [PubMed: 10813780]

Ghashghaei HT, Barbas H. Pathways for emotion: interactions of prefrontal and anterior temporal pathways in the amygdala of the rhesus monkey. Neuroscience. 2002; 115:1261–1279. [PubMed: 12453496]

Goodwin RD, Fergusson DM, Horwood LJ. Early anxious/withdrawn behaviours predict later internalising disorders. J.Child Psychol.Psychiatry. 2004; 45:874–883. [PubMed: 15056317]

Gosch A, Pankau R. Social-emotional and behavioral adjustment in children with Williams-Beuren syndrome. Am.J.Med.Genet. 1994; 53:335–339. [PubMed: 7864042]

Hariri AR, Drabant EM, Munoz KE, Kolachana BS, Mattay VS, Egan MF, Weinberger DR. A susceptibility gene for affective disorders and the response of the human amygdala. Arch.Gen.Psychiatry. 2005; 62:146–152. [PubMed: 15699291]

Hariri AR, Mattay VS, Tessitore A, Kolachana B, Fera F, Goldman D, Egan MF, Weinberger DR. Serotonin transporter genetic variation and the response of the human amygdala. Science. 2002; 297:400–403. [PubMed: 12130784]

Hoeft F, Barnea-Goraly N, Haas BW, Golarai G, Ng D, Mills D, Korenberg J, Bellugi U, Galaburda A, Reiss AL. More is not always better: increased fractional anisotropy of superior longitudinal fasciculus associated with poor visuospatial abilities in Williams syndrome. J.Neurosci. 2007; 27:11960–11965. [PubMed: 17978036]

Hua K, Zhang J, Wakana S, Jiang H, Li X, Reich DS, Calabresi PA, Pekar JJ, van Zijl PC, Mori S. Tract probability maps in stereotaxic spaces: analyses of white matter anatomy and tract-specific quantification. Neuroimage. 2008; 39:336–347. [PubMed: 17931890]

Indovina I, Robbins TW, Nunez-Elizalde AO, Dunn BD, Bishop SJ. Fear-conditioning mechanisms associated with trait vulnerability to anxiety in humans. Neuron. 2011; 69:563–571. [PubMed: 21315265]

Jbabdi S, Woolrich MW, Andersson JL, Behrens TE. A Bayesian framework for global tractography. Neuroimage. 2007; 37:116–129. [PubMed: 17543543]

Kagan J, Reznick JS, Snidman N. Temperamental influences on reactions to unfamiliarity and challenge. Adv.Exp.Med.Biol. 1988; 245:319–339. [PubMed: 3228020]

Kaufman, A.; Kaufman, N. Circle Pines, NM: American Guicance Services, Inc.; 1990. Kaufman Brief Intelligence Test.

Kessler RC, Chiu WT, Demler O, Merikangas KR, Walters EE. Prevalence, severity, and comorbidity of 12-month DSM-IV disorders in the National Comorbidity Survey Replication. Arch.Gen.Psychiatry. 2005; 62:617–627. [PubMed: 15939839]

Klein-Tasman BP, Mervis CB. Distinctive personality characteristics of 8-, 9-, and 10-year-olds with Williams syndrome. Dev.Neuropsychol. 2003; 23:269–290. [PubMed: 12730028]

Lancaster JL, Rainey LH, Summerlin JL, Freitas CS, Fox PT, Evans AC, Toga AW, Mazziotta JC. Automated labeling of the human brain: a preliminary report on the development and evaluation of a forward-transform method. Hum.Brain Mapp. 1997; 5:238–242. [PubMed: 20408222]

Lancaster JL, Woldorff MG, Parsons LM, Liotti M, Freitas CS, Rainey L, Kochunov PV, Nickerson D, Mikiten SA, Fox PT. Automated Talairach atlas labels for functional brain mapping. Hum.Brain Mapp. 2000; 10:120–131. [PubMed: 10912591]

Leyfer O, Woodruff-Borden J, Mervis CB. Anxiety disorders in children with Williams syndrome, their mothers, and their siblings: implications for the etiology of anxiety disorders. J.Neurodev.Disord. 2009; 1:4–14. [PubMed: 20161441]

Leyfer OT, Woodruff-Borden J, Klein-Tasman BP, Fricke JS, Mervis CB. Prevalence of psychiatric disorders in 4 to 16-year-olds with Williams syndrome. Am.J.Med.Genet.B Neuropsychiatr.Genet. 2006; 141B:615–622. [PubMed: 16823805]

Liotti M, Mayberg HS, Brannan SK, McGinnis S, Jerabek P, Fox PT. Differential limbic--cortical correlates of sadness and anxiety in healthy subjects: implications for affective disorders. Biol.Psychiatry. 2000; 48:30–42. [PubMed: 10913505]

Maldjian JA, Laurienti PJ, Burdette JH. Precentral gyrus discrepancy in electronic versions of the Talairach atlas. Neuroimage. 2004; 21:450–455. [PubMed: 14741682]

Maldjian JA, Laurienti PJ, Kraft RA, Burdette JH. An automated method for neuroanatomic and cytoarchitectonic atlas-based interrogation of fMRI data sets. Neuroimage. 2003; 19:1233–1239. [PubMed: 12880848]

Marenco S, Siuta MA, Kippenhan JS, Grodofsky S, Chang WL, Kohn P, Mervis CB, Morris CA, Weinberger DR, Meyer-Lindenberg A, Pierpaoli C, Berman KF. Genetic contributions to white matter architecture revealed by diffusion tensor imaging in Williams syndrome. Proc.Natl.Acad.Sci.U.S.A. 2007; 104:15117–15122. [PubMed: 17827280]

Merla G, Brunetti-Pierri N, Micale L, Fusco C. Copy number variants at Williams-Beuren syndrome 7q11.23 region. Hum.Genet. 2010; 128:3–26. [PubMed: 20437059]

Meyer-Lindenberg A, Hariri AR, Munoz KE, Mervis CB, Mattay VS, Morris CA, Berman KF. Neural correlates of genetically abnormal social cognition in Williams syndrome. Nat.Neurosci. 2005; 8:991–993. [PubMed: 16007084]

Mori, S.; Wakana, S.; van Zijl, PCM.; Nagae-Poetscher, LM. MRI Atlas of Human White Matter. 1st ed.. Amsterdam, The Netherlands, San Diego, CA: Elsevier; 2004.

Munoz KE, Meyer-Lindenberg A, Hariri AR, Mervis CB, Mattay VS, Morris CA, Berman KF. Abnormalities in neural processing of emotional stimuli in Williams syndrome vary according to social vs. non-social content. Neuroimage. 2010; 50:340–346. [PubMed: 20004252]

Ochsner KN, Ray RD, Cooper JC, Robertson ER, Chopra S, Gabrieli JD, Gross JJ. For better or for worse: neural systems supporting the cognitive down- and up-regulation of negative emotion. Neuroimage. 2004; 23:483–499. [PubMed: 15488398]

Oldfield RC. The assessment and analysis of handedness: the Edinburgh inventory. Neuropsychologia. 1971; 9:97–113. [PubMed: 5146491]

Ongur D, Drevets WC, Price JL. Glial reduction in the subgenual prefrontal cortex in mood disorders. Proc.Natl.Acad.Sci.U.S.A. 1998; 95:13290–13295. [PubMed: 9789081]

Pezawas L, Meyer-Lindenberg A, Drabant EM, Verchinski BA, Munoz KE, Kolachana BS, Egan MF, Mattay VS, Hariri AR, Weinberger DR. 5-HTTLPR polymorphism impacts human cingulate-amygdala interactions: a genetic susceptibility mechanism for depression. Nat.Neurosci. 2005; 8:828–834. [PubMed: 15880108]

Phan KL, Fitzgerald DA, Nathan PJ, Moore GJ, Uhde TW, Tancer ME. Neural substrates for voluntary suppression of negative affect: a functional magnetic resonance imaging study. Biol.Psychiatry. 2005; 57:210–219. [PubMed: 15691521]

Reiss AL, Eckert MA, Rose FE, Karchemskiy A, Kesler S, Chang M, Reynolds MF, Kwon H, Galaburda A. An experiment of nature: brain anatomy parallels cognition and behavior in Williams syndrome. J.Neurosci. 2004; 24:5009–5015. [PubMed: 15163693]

Reznick JS, Hegeman IM, Kaufman ER, Woods SW, Jacobs M. Retrospective and concurrent self-report of behavioral inhibition and their relation to adult mental health. Development and Psychopathology. 1992; 4:301–321.

Schwartz CE, Snidman N, Kagan J. Adolescent social anxiety as an outcome of inhibited temperament in childhood. J.Am.Acad.Child Adolesc.Psychiatry. 1999; 38:1008–1015. [PubMed: 10434493]

Smith SM. Fast robust automated brain extraction. Hum.Brain Mapp. 2002; 17:143–155. [PubMed: 12391568]

Smith SM, Jenkinson M, Johansen-Berg H, Rueckert D, Nichols TE, Mackay CE, Watkins KE, Ciccarelli O, Cader MZ, Matthews PM, Behrens TE. Tract-based spatial statistics: voxelwise analysis of multi-subject diffusion data. Neuroimage. 2006; 31:1487–1505. [PubMed: 16624579]

Smith SM, Jenkinson M, Woolrich MW, Beckmann CF, Behrens TE, Johansen-Berg H, Bannister PR, De LM, Drobnjak I, Flitney DE, Niazy RK, Saunders J, Vickers J, Zhang Y, De SN, Brady JM, Matthews PM. Advances in functional and structural MR image analysis and implementation as FSL. Neuroimage. 2004; 23 Suppl 1:S208–S219. [PubMed: 15501092]

Smoller JW, Yamaki LH, Fagerness JA, Biederman J, Racette S, Laird NM, Kagan J, Snidman N, Faraone SV, Hirshfeld-Becker D, Tsuang MT, Slaugenhaupt SA, Rosenbaum JF, Sklar PB. The corticotropin-releasing hormone gene and behavioral inhibition in children at risk for panic disorder. Biol.Psychiatry. 2005; 57:1485–1492. [PubMed: 15953484]

Stefanacci L, Amaral DG. Some observations on cortical inputs to the macaque monkey amygdala: an anterograde tracing study. J.Comp Neurol. 2002; 451:301–323. [PubMed: 12210126]

Stinton C, Elison S, Howlin P. Mental health problems in adults with Williams syndrome. Am.J.Intellect.Dev.Disabil. 2010; 115:3–18. [PubMed: 20025356]

Thornton-Wells TA, Avery SN, Blackford JU. Using novel control groups to dissect the amygdala's role in Williams Syndrome. Developmental Cognitive Neuroscience. 2011; 1(3):295–304. [PubMed: 21731599]

Tzourio-Mazoyer N, Landeau B, Papathanassiou D, Crivello F, Etard O, Delcroix N, Mazoyer B, Joliot M. Automated anatomical labeling of activations in SPM using a macroscopic anatomical parcellation of the MNI MRI single-subject brain. Neuroimage. 2002; 15:273–289. [PubMed: 11771995]

Wakana S, Caprihan A, Panzenboeck MM, Fallon JH, Perry M, Gollub RL, Hua K, Zhang J, Jiang H, Dubey P, Blitz A, van ZP, Mori S. Reproducibility of quantitative tractography methods applied to cerebral white matter. Neuroimage. 2007; 36:630–644. [PubMed: 17481925]

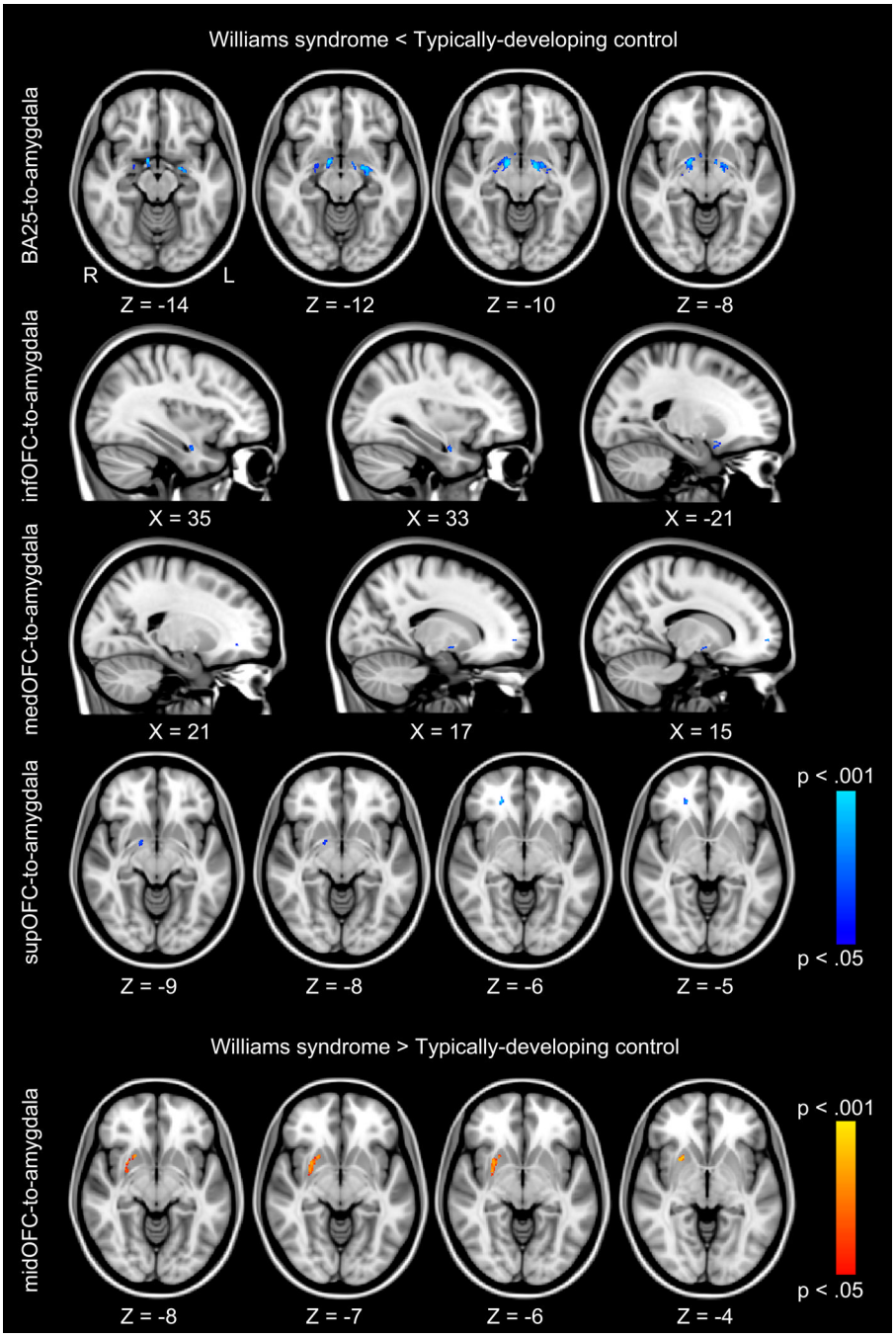

Fig. 1.

Tractography analysis of prefrontal-amygdala pathways. Blue clusters represent white matter regions where individuals with Williams syndrome have significantly lower fractional anisotropy (FA) values, $p < .05$, family-wise error (FWE) corrected for multiple comparisons than typically-developing controls. Red clusters represent white matter regions where individuals with Williams syndrome have significantly higher FA values ($p < .05$, FWE corrected) than typically-developing controls. Anatomically, FA differences are located bilaterally within the ventral amygdalofugal pathway, the uncinate fasciculus, the inferior longitudinal fasciculus, and the inferior fronto-occipital fasciculus. FA differences are overlaid onto the MNI-152 T1-weighted standard brain. Subgenual anterior cingulate

(BA25); inferior orbitofrontal cortex (infOFC); medial orbitofrontal cortex (medOFC); middle orbitofrontal cortex (midOFC); superior orbitofrontal cortex (supOFC).

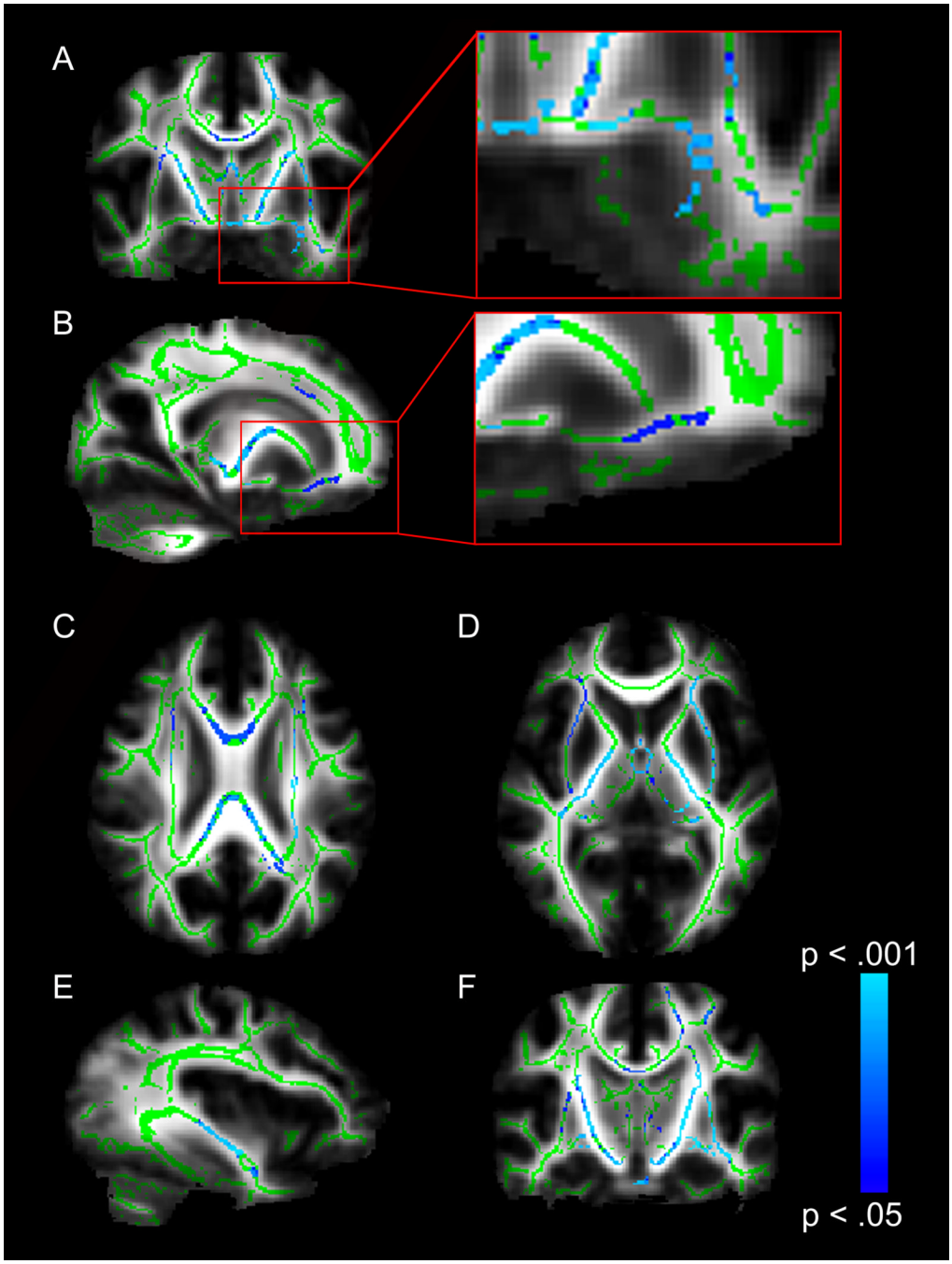

Fig. 2.

TBSS analysis of whole-brain white matter differences. Blue voxels represent white matter regions where individuals with Williams syndrome (WS) have lower fractional anisotropy (FA) values ($p < .05$, FWE corrected) than typically-developing controls. Voxels are overlaid on the TBSS white matter skeleton (green) and the FMRIB-58 FA standard brain (grayscale). **(A)** Coronal image showing lower FA in individuals with WS in the left ventral amygdalofugal pathway. **(B)** Sagittal image showing lower FA in individuals with WS in the right uncinate fasciculus pathway. **(C)** Axial image showing lower FA in individuals with WS in the corpus callosum. **(D)** Axial image showing lower FA in individuals with WS in bilateral external capsules and bilateral posterior limbs of the internal capsule. **(E)** Sagittal

image showing lower FA in individuals with WS in the inferior fronto-occipital fasciculus. **(F)** Coronal image showing lower FA in individuals with WS in bilateral corticospinal tracts.

Table 1

Demographic, temperament, and clinical characteristics for Williams Syndrome subjects and typically-developing controls.

		Typically-Developing Control (TDC) *n* = 9		Williams Syndrome (WS) *n* = 8		TDC vs. WS
		Mean	**SD**	**Mean**	**SD**	**t-test *p* value**
Age (years)		25	6.36	22	3.51	.38
IQ		117	14.27	78	20.16	.002 *
Temperament						
Retrospective	(RSRI)					
Social		3.91	.34	1.92	.63	< .001 *
Nonsocial		3.65	.72	2.19	.76	.003 *
Adult	(ASRI)					
Social		2.94	.46	1.71	.39	< .001 *
Nonsocial		2.76	.54	2.46	.52	.36
		n		***n***		**Chi-Square *p* value**
Gender	(%M)[a]	56%		75%		.40
Race	(C:AA:A)[b]	7:1:1		8:0:0		.37
Handedness	(%R)[c]	67%		75%		.08

* $p < .05$

[a] M = Male;

[b] C = Caucasian, AA = African American, A = Asian;

[c] R = Right

Table 2

Peak voxel responses listed by prefrontal-amygdala tract and group contrast.

Tractography Mask		Fiber Pathway	# Voxels	t	X	Y	Z
Williams Syndrome < Typically-Developing Control							
BA25-to-Amygdala							
	Left	VAF	535	5.64	−13	−6	−10
	Right	VAF/UF	530	5.94	14	−4	−11
			30	5.09	6	6	−9
			19	4.09	32	−2	−23
infOFC-to-Amygdala							
	Left	UF/ILF	32	5.22	−21	10	−15
	Right	UF/ILF	105	4.37	35	−3	−24
medOFC-to-Amygdala							
	Right	VAF/ILF/IFO	73	6.04	14	−3	−11
			28	6.45	15	59	−1
			8	6.34	21	39	−6
supOFC-to-Amygdala							
	Right	VAF/ILF/IFO	45	6.56	22	38	−6
			37	5.22	14	−2	−10
			15	5.31	11	0	−12
Williams Syndrome > Typically-Developing Control							
midOFC-to-Amygdala							
	Right	IFO	280	5.07	25	11	−3

Note: Statistical significance was determined by a voxelwise $p < .05$, family-wise error corrected for multiple comparisons. Brodmann Area 25 (BA25); Inferior Orbitofrontal Cortex (infOFC); Medial Orbitofrontal Cortex (medOFC); Middle Orbitofrontal Cortex (midOFC); Superior Orbitofrontal Cortex (supOFC); Inferior Fronto-Occipital Fasciculus (IFO); Inferior Longitudinal Fasciculus (ILF); Uncinate Fasciculus (UF); Ventral Amygdalofugal Pathway (VAF). Peak voxel locations (X, Y, Z) are listed in MNI space.